Chemistry–A European Journal

Supporting Information

Formation of Highly Ordered Molecular Porous 2D Networks from Cyano-Functionalized Porphyrins on Cu(111)

Rajan Adhikari,[a] Gretel Siglreithmaier,[a] Martin Gurrath,[b] Manuel Meusel,[a] Jan Kuliga,[a] Michael Lepper,[a] Helen Hölzel,[c] Norbert Jux,[c] Bernd Meyer,*[b] Hans-Peter Steinrück,*[a] and Hubertus Marbach[a]

Experimental Section

STM. All experiments, sample preparations and STM measurements were performed in an ultrahigh vacuum (UHV) system with a base pressure in the low 10^{-10} mbar regime. The preparation of the Cu(111) surface was done by sequential cycles of Ar^+ ions bombardment (600 eV) followed by annealing at 850 K. STM was performed with an RHK UHV VT STM 300 operated at room temperature (RT) with RHK SPM 100 electronics. All STM images were obtained with a manually cut Pt/Ir tip in constant current mode. The bias voltage referred to the sample. The STM images were processed with the WSxM software.[1] For noise reduction, moderate filtering (background subtraction, Gaussian smoothing) was applied. The investigated porphyrin derivatives, Cu-TCNPP, Cu-*cis*DCNPP and 2H-*cis*DCNPP were deposited onto the substrate held at RT using a home-built Knudsen cell, with the crucible at 790, 675 and 645 K, respectively. The azimuthal orientation of the Cu(111) surface was determined through the diffusion direction of 2H-TPP along the $\langle\bar{1}10\rangle$ high-symmetry crystallographic axes at RT.[2]

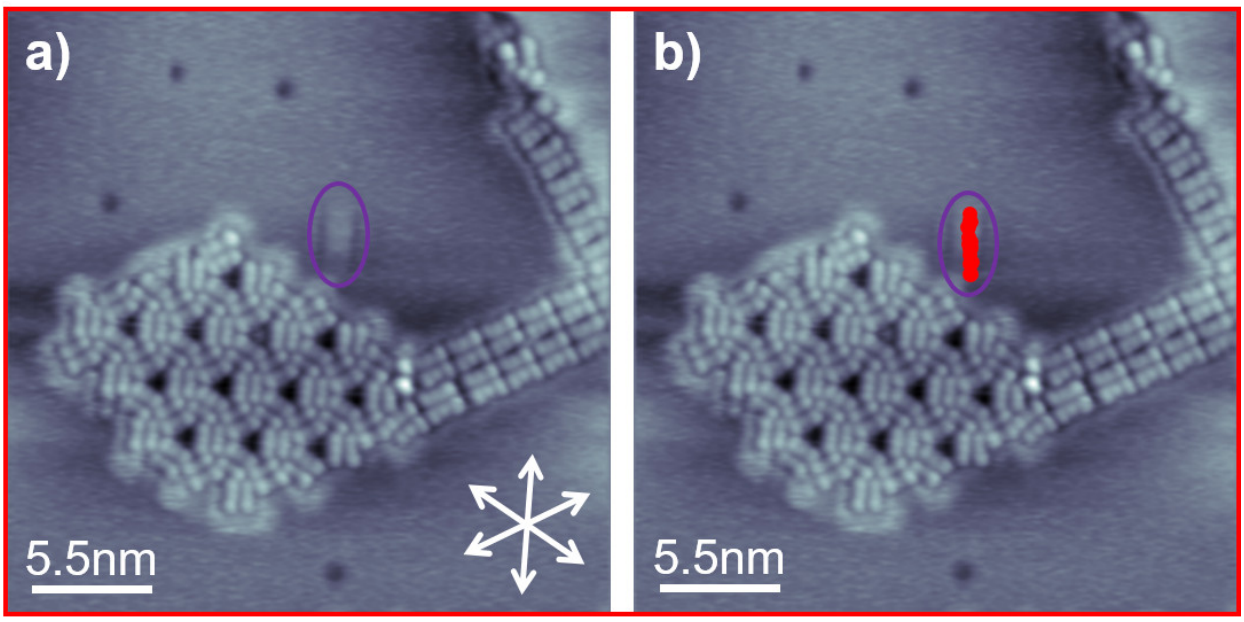

Figure S1: Average frame of an STM movie (15 consecutively recorded images) of Cu-TCNPP, deposited and measured at RT ($27.5 \times 27.5\,nm^2$, U_{bias} = -1 V, I_{set} = 28.8 pA). A mobile metal-free 2H-TCNPP molecule diffusing along a high-symmetry crystallographic direction of the Cu(111) surface is marked in red and by a purple solid oval.

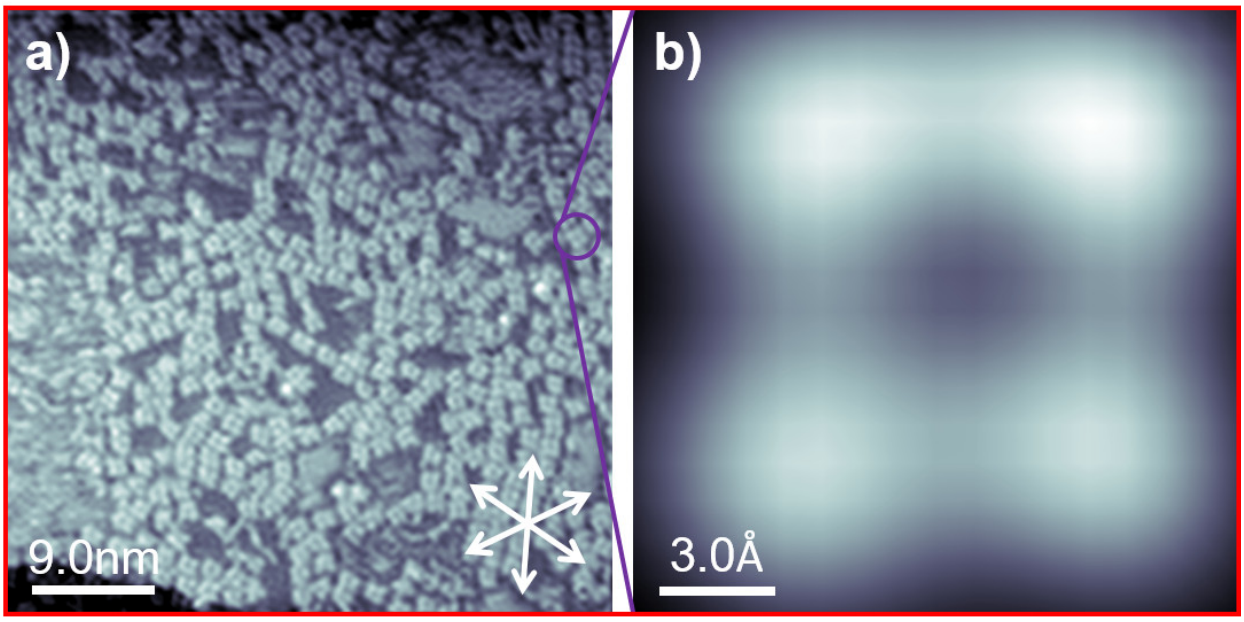

Figure S2: (a) The STM overview image ($45 \times 45\,\mathrm{nm}^2$), acquired at RT after annealing at 450 K, shows the loss of 2D long-range order and the appearance of randomly distributed individual molecules. (b) Magnified STM image of a single Cu-TCNPP molecule, which shows the change in appearance from six to four pronounced protrusions promoted by the annealing step ($1.5 \times 1.5\,\mathrm{nm}^2$, U_{bias} = -1 V, I_{set} = 30.3 pA).

Synthesis. All chemicals were purchased from Sigma-Aldrich®, Acros Organics®, Fluka®, Fisher Scientific® or Alfa Aesar® and used without further purification. Pyrrole, benzaldehyde and solvents for chromatography were distilled prior to usage. HPLC solvents were used for synthesis. Dichloromethane was distilled from K_2CO_3. High resolution mass spectrometry was performed on a Bruker maXis 4G UHR MS/MS or a Bruker micrOTOF II focus TOF MS spectrometer. Microwave-assisted reactions were carried out in a Biotage®initiator$_+$ monomode microwave reactor and its respective vials. Standard stirring rate was 600 rpm, fixed hold time (FHT) was on, and no external cooling was applied.

The free-base porphyrins were synthesized as reported earlier.[3,4] The metalation of the porphyrins was done by the following general procedure: The free-base porphyrin was dissolved in $CHCl_3$ and stirred at room temperature. A saturated solution of $Cu(OAc)_2$ in CH_3OH was added. The mixture was stirred overnight at room temperature. The solvent was removed under reduced pressure. The crude product was purified by plug filtration (SiO_2, diameter: 3.5 cm, length: 7 cm, CH_2Cl_2), yielding the metalated porphyrins as dark red solids. For further details (yields, etc.), please see the corresponding product data below.

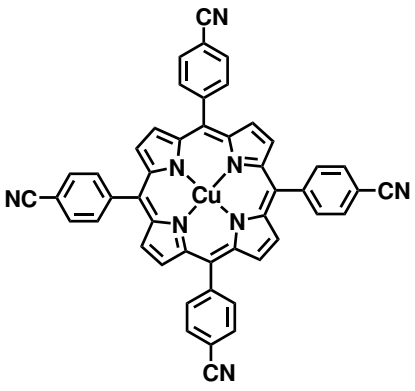

$C_{48}H_{24}CuN_8$
M = 776.32 g/mol

Cu-TCNPP

The free-base porphyrin (0.040 g; 0.056 mmol) was dissolved in 10 mL $CHCl_3$. 10 mL of the saturated solution $Cu(OAc)_2$ in CH_3OH were used.

Yield: 80 % (0.035 g; 0.045 mmol)

HRMS (APPI, ACN/CH_2Cl_2): m/z calc. for $C_{48}H_{24}CuN_8$ [M^+]: 775.1414; found: 775.1419

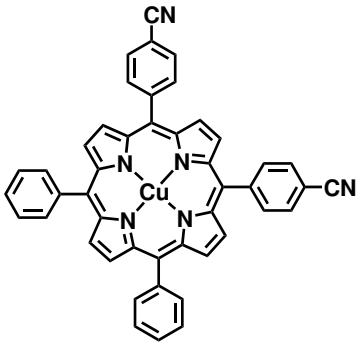

$C_{46}H_{26}CuN_6$
M = 726.30 g/mol

Cu-cisDCNPP

The free-base porphyrin (0.010 g; 0.015 mmol) was dissolved in 3 mL $CHCl_3$. 3 mL of the saturated solution $Cu(OAc)_2$ in CH_3OH were used.

Yield: 100 % (0.011 g; 0.015 mmol)

HRMS (APPI, ACN/CH_2Cl_2): m/z calc. for $C_{46}H_{26}CuN_6$ [M^+]: 725.1509; found: 725.1508

Figure S3: High-resolution mass spectra of Cu-TCNPP. Measured (top) and calculated (bottom) isotope pattern of the molecular ion peak.

Figure S4: High-resolution mass spectra of Cu-*cis*DCNPP. Measured (top) and calculated (bottom) isotope pattern of the molecular ion peak.

DFT Calculations

Spin-polarized DFT calculations were performed with the periodic plane-wave code `PWscf` of the Quantum Espresso software package.[5] The gradient-corrected PBE exchange-correlation functional of Perdew, Burke and Ernzerhof,[6] Vanderbilt ultrasoft pseudopotentials,[7] and a plane-wave basis set with a energy cutoff of 30 Ry were used. Dispersion corrections to PBE energies and forces were included by our D3$^{\text{surf}}$ scheme.[8,9] D3$^{\text{surf}}$ is an extension of the original D3 method proposed by Grimme et al.[10,11], in which the parameter set of coordination-dependent C_6 coefficients is extended by additional values for the substrate atoms at higher coordination numbers of the surface and bulk atoms.[8,9]

Cu(111) surfaces were represented by periodically repeated slabs with a thickness of three atomic layers. The calculations for single, non-interacting porphyrin molecules were done with a hexagonal (10×10) surface unit cell (300 Cu atoms). $(7\sqrt{3}\times7\sqrt{3})$R30° (441 Cu atoms) and $(8\sqrt{3}\times8\sqrt{3})$R30° (576 Cu atoms) unit cells containing three porphyrin molecules were used in the studies of porous hexagonal honeycomb-type adsorbate layers. The calculated PBE+D3$^{\text{surf}}$ bulk lattice constant of Cu of 3.606 Å was chosen for the lateral extensions of the slabs. The atoms in the Cu bottom layer were kept fixed, and only the two upper layers together with the adsorbate were relaxed in the geometry optimizations using a force convergence threshold of 3 meV/Å. Well-converged structures and adsorption energies were obtained with a (2,2,1) Monkhorst-Pack k-point mesh together with a Gaussian smearing with a smearing width of 0.02 Ry.[3]

In the calculation of the energy profile (the potential energy surface for Cu-TPP displacement and diffusion), the lateral coordinates of the Cu atoms were kept fixed at their ideal positions and only the vertical coordinate was relaxed for the different porphyrin positions. At each point of the energy profile, the lateral coordinates of the central Cu atom of the porphyrin molecule were constrained to the respective value and all other coordinates (including the distance of the Cu atom from the surface) were relaxed.

1) Adsorption Site of CN-Functionalized Cu Porphyrins on Cu(111)

In the gas phase, Cu porphyrins adopt the saddle-shape conformation with $D_{2\text{d}}$ symmetry: two opposite pyrrole rings are tilted up, the other two are tilted down. This alternating up and down tilt of the pyrrole rings is accompanied by an alternate left and right rotation of the outer phenyl units. The ruffled geometry with S_4 symmetry, in which the pyrrole rings are not tilted but rotated alternately to the left and to the right, is slightly higher in energy.

To entangle the interaction of the porphyrin core with the Cu surface from the site-specific adsorption of terminal CN groups, we determined first the preferred adsorption site for Cu-

TPPs without cyano functionalization. Four different adsorption sites were probed, with the central Cu atom of the porphyrin sitting on-top of a surface Cu atom, above an fcc or hcp hollow site, and for a bridging position. Furthermore, two orientations were considered: either the two downward- or the two upward-tilted pyrrole rings were aligned along the main [110]-direction, i.e., the densely-packed Cu rows. Both orientations are related to each other by rotating the Cu-TPP by 90° or by flipping the Cu-TPP upside down. The global energy minimum is found for the bridge position and the orientation with the downward-tilted pyrrole rings along the Cu rows (see Figure S5a). This orientation is in agreement with the observed appearance of the Cu porphyrins in STM: the downward-tilted pyrrole rings give rise to a dark line along the Cu rows, whereas the upward-tilted pyrroles perpendicular to the Cu rows together with the four phenyl rings are seen as three bright protrusions above and below the dark line (see Figure 2c in the manuscript). As binding energy of single Cu-TPPs on Cu(111) we obtain a value of 3.39 eV. This is only slightly smaller than the binding energy of 3.58 eV for free-base 2H-TPPs on Cu(111) with inverted adsorption geometry[12] (calculated by the same PBE+D3$^{\mathrm{surf}}$ approach). The binding site and the molecular orientation of Cu-TPP on Cu(111) are mainly determined by the position of the central N atoms. Figure S5a shows that all four nitrogens are above substrate Cu atoms, with a better match for the two N atoms of the upward-tilted pyrrole rings. Furthermore, these two N atoms are slightly below the central Cu atom of the porphyrin (thereby reducing the distance to the Cu atoms of the surface), whereas the two N atoms of the downward-tilted pyrroles are slightly above. A rotation of the Cu-TPP by 90° inverts the up-down pattern of the N atoms. This reduces the Cu-TPP binding energy by 0.15 eV, which demonstrates the importance of the N–Cu interactions. Of the other adsorption sites, the fcc and hcp hollow positions are unstable. The Cu-TPP molecules relax to the bridge position in the geometry optimization (see Figure S6b). The on-top site is metastable and represents the least favorable position for the Cu-TPP. Compared to the global energy minimum structure, the binding energy is reduced by 0.35 and 0.14 eV for the orientation with the downward-tilted pyrrole rings parallel and perpendicular to the Cu rows, respectively.

After having identified the preferred surface site for the Cu porphyrin core, we now add terminal CN groups. Previous DFT calculations have shown that HCN molecules bind with their N-side exclusively to on-top positions of the Cu(111) surface; when the D3 dispersion correction is not included in the DFT calculation, fcc, hcp and bridge sites are repulsive.[3] We start from the global optimum structure of the non-functionalized Cu-TPP molecule (see Figure S5a) and add four CN groups. As shown in Figure S6a, the CN groups nicely point toward the Cu atoms of the surface. In the subsequent geometry optimization the CN groups just bend down and establish their favored CN–Cu contact (see Figure S6b) with a N–Cu distance of 2.07 Å. Thus, having the porphyrin core at its most favorable adsorption site automatically guarantees that also added terminal CN groups can bind to the Cu surface in their preferred binding mode.

Figure S7a shows the relaxed structure when only two CN groups are added to the Cu-TPP. Here the porphyrin core is slightly pushed out of its preferred bridge site by about 0.4 Å. Obviously, the match between the position of the terminating CN groups and the surface Cu atoms is good, but not perfect. The energy landscape for shifting a Cu-TPP out of its

bridge site along the mirror symmetry plane (see Figure S5b) has a sinusoidal shape. The energy cost for a displacement of 0.4 Å is only about 0.03 eV. However, as a consequence of this small mismatch we have to expect that the Cu-TCNPP with four terminal CN groups, which has to stay in the bridge position, is slightly strained. Indeed, this is seen when we analyze the binding energies (see Table S1). The binding energy of the Cu-*cis*DCNPP molecule is 0.21 eV larger than for the non-functionalized Cu-TPP. We can attribute this gain of binding energy to the interaction of the CN groups with the surface. Taking into account that we have "lost" 0.03 eV in binding energy by displacing the porphyrin from the ideal bridge position, we can assign an interaction energy $E_{\mathrm{int}}^{\mathrm{CN}}$ of about 0.12 eV to each CN–Cu contact. Based on this value for $E_{\mathrm{int}}^{\mathrm{CN}}$ we would expect an increase in binding energy of 0.48 eV for the Cu-TCNPP with its four CN groups. However, from the DFT calculations we only obtain 0.40 eV. The small difference of about 0.08 eV is the strain energy, which is induced by the requirement that now all four CN groups connect to on-top Cu sites and the porphyrin core has to remain strictly in the bridge position.

Finally, we turn to the Cu adatoms. They occupy the fcc and hcp hollow sites on the Cu(111) surface. According to our DFT calculations their formation energy

$$E_{\mathrm{f}}^{\mathrm{Cu\text{-}ad}} = E_{\mathrm{slab}}^{\mathrm{Cu\text{-}ad}} - E_{\mathrm{slab}}^{\mathrm{Cu(111)}} - E_{\mathrm{bulk}}^{\mathrm{Cu}}$$

is about 0.82 eV for both sites. $E_{\mathrm{slab}}^{\mathrm{Cu\text{-}ad}}$ and $E_{\mathrm{slab}}^{\mathrm{Cu(111)}}$ are the total energies of a Cu(111) slab with and without a Cu adatom and $E_{\mathrm{bulk}}^{\mathrm{Cu}}$ is the energy of a Cu bulk unit cell. Figure S6c shows an initial structure derived from the relaxed Cu-TPP molecule with *ad hoc* added CN groups and Cu adatoms. As in the case without adatoms, a very good geometrical match can be seen. In the geometry optimization the CNs readjust and establish a firm contact to the Cu adatoms with a N–Cu distance of 1.89 Å (see Figure S6d). Several other positions of the Cu adatoms were considered in the calculations, but they were all less favorable. Figures S7b+c show the relaxed structures for Cu-*cis*DCNPP and Cu-TCNPP when only two Cu adatoms are attached. In the case of Cu-*cis*DCNPP in Figure S7b, no displacement of the porphyrin core from the bridge site is visible, i.e., the geometrical match between the terminal CN groups and the adatoms is perfect and no strain is induced. On the other hand, for Cu-TCNPP in Figure S7c, the CN–Cu contact to Cu atoms of the terrace induces a small shift of the porphyrin toward the Cu adatoms.

For all structures with Cu adatoms the porphyrin binding energy was calculated according to

$$E_{\mathrm{b}} = E_{\mathrm{slab}}^{\mathrm{Cu(111)}} + N_{\mathrm{ad}}^{\mathrm{Cu}}\, E_{\mathrm{bulk}}^{\mathrm{Cu}} + E_{\mathrm{mol}}^{\mathrm{porph}} - E_{\mathrm{slab}}^{\mathrm{porph/Cu\text{-}ad}} \quad ,$$

which includes the energy that is required to form the Cu adatoms.[13] $N_{\mathrm{ad}}^{\mathrm{Cu}}$ is the number of Cu adatoms in the structure and $E_{\mathrm{mol}}^{\mathrm{porph}}$ is the gas-phase energy of the porphyrin. The calculated porphyrin binding energies with and without Cu adatoms are surprisingly similar (see Table S1). This means that the stronger interaction of the CN groups with the Cu adatoms almost exactly compensates the energy cost of creating the adatoms. However, the binding energies of the structures with adatoms are systematically smaller by a small margin. This means that the adatom structures with single molecules are thermodynamically unstable and should decompose into adsorbed molecules on the terrace and condensed Cu atoms at zero temperature unless hindered by kinetic effects.

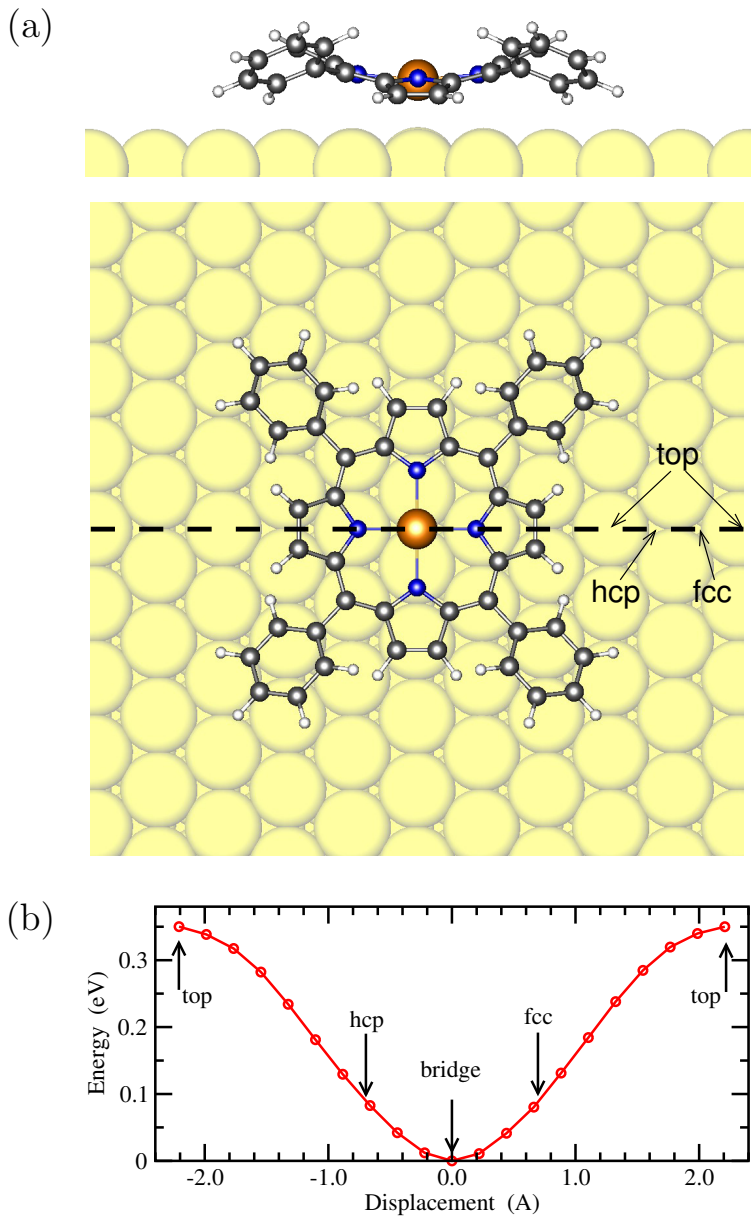

Figure S5: (a) Side and top view of the relaxed structure of a single Cu-TPP molecule on Cu(111) at its most favorable adsorption site. The saddle shape of the porphyrin is visible. The downward-tilted pyrrole rings (with slightly higher N atoms) are oriented along the densely-packed Cu rows. The black dashed line indicates the mirror symmetry plane. Cu, C, N and H atoms are shown in yellow, black, blue and white, respectively. The same color code is used in all figures. (b) Energy profile for the shift of Cu-TPP along the mirror symmetry line.

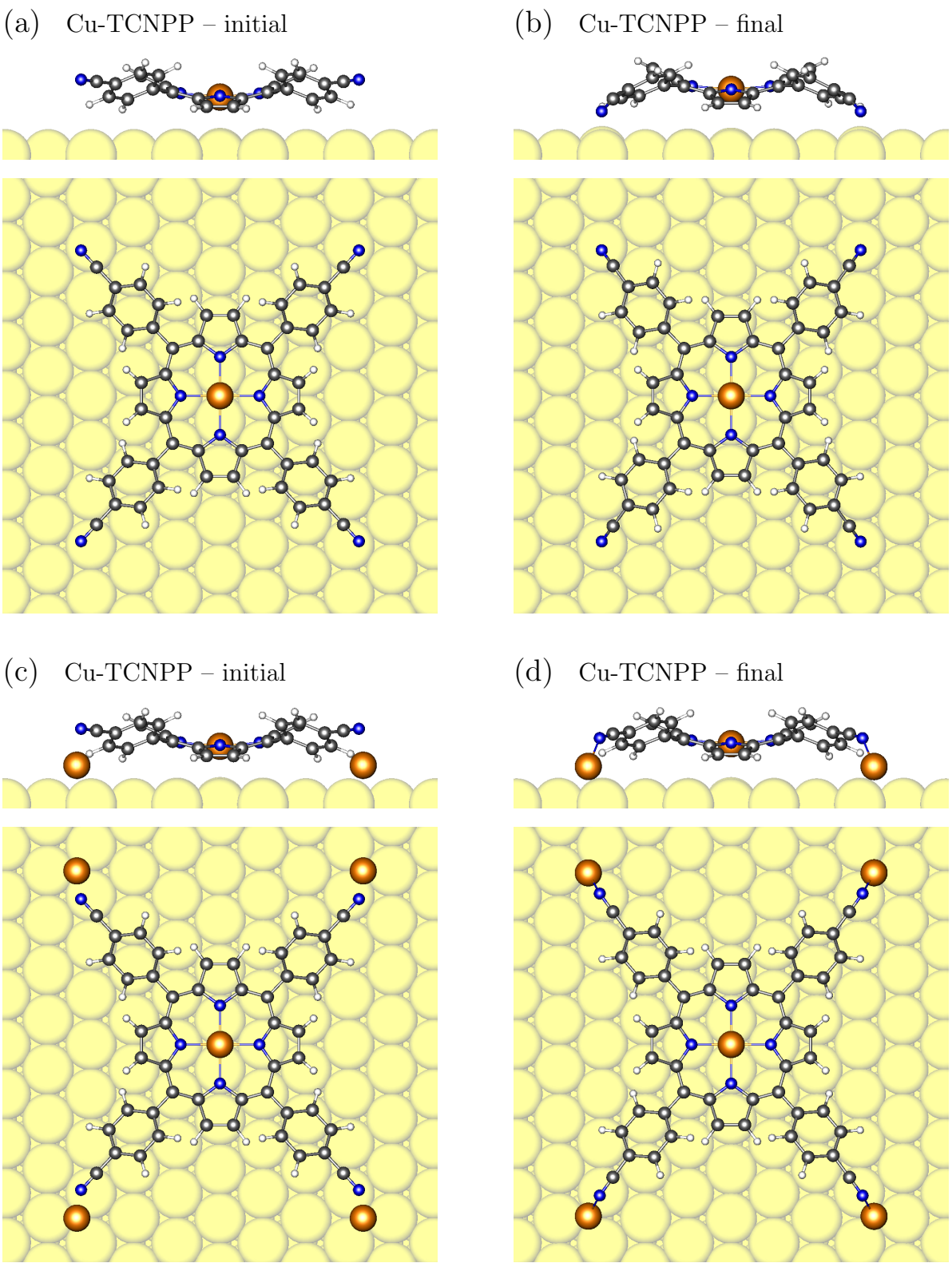

Figure S6: Side and top views of a single Cu-TCNPP molecule on Cu(111), (a,b) without and (c,d) with Cu adatoms. (a,c) show the relaxed structure of Cu-TPP from Figure S5a with *ad hoc* added CN groups. The porphyrin core is at its preferred adsorption site, simultaneously all CN groups point to a Cu on-top site or can easily connect to a Cu adatom. The final structures after geometry optimization are shown in (b,d).

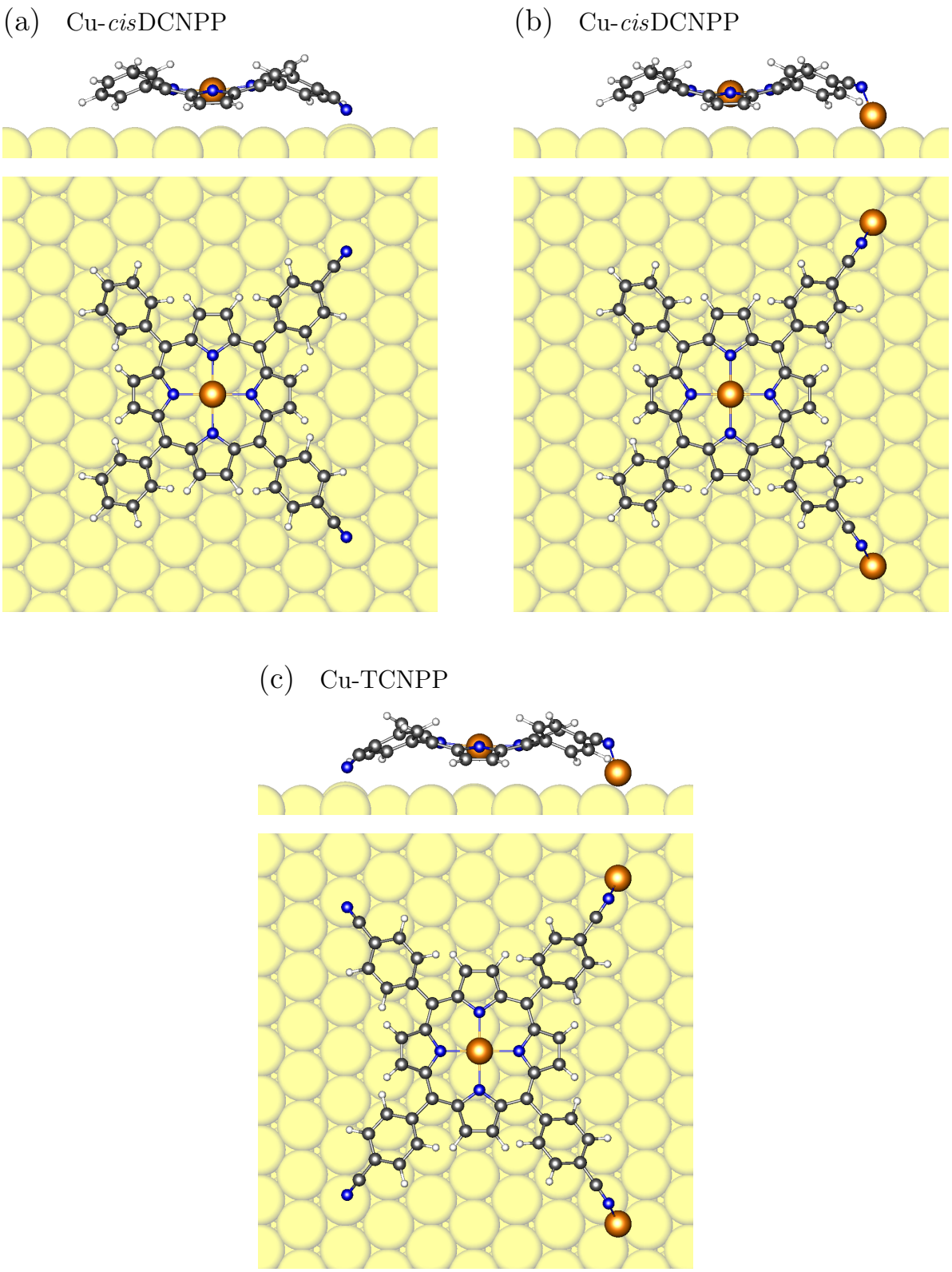

Figure S7: Side and top views of the relaxed structure of a single (a,b) Cu-*cis*DCNPP and (c) Cu-TCNPP molecule on Cu(111) without (a) and with two Cu adatoms (b,c). The mirror symmetry is preserved in all structures. If CN groups bind to the Cu substrate, the porphyrin core is slightly pushed out of its favored bridge position (a,c), whereas binding to Cu adatoms does not have this effect (b).

Table S1: Calculated binding energy E_b of single, well-separated Cu porphyrins on Cu(111). ΔE_b is the change in binding energy with respect to non-functionalized Cu-TPP. $E_\mathrm{int}^\mathrm{CN}$ is the interaction energy per terminal CN group with the Cu surface (first entry: with Cu atoms of the terrace, second entry: with Cu adatoms). Except where otherwise noted, $E_\mathrm{int}^\mathrm{CN}$ is given by ΔE_b divided by the number of CNs. Δd is the displacement of the porphyrin out of the bridge position.

Porphyrin	E_b (eV)	ΔE_b (eV)	$E_\mathrm{int}^\mathrm{CN}$ (eV)	Δd (Å)
Cu-TPP	3.39			–
Cu-*cis*DCNPP		+0.21	+0.12 [a] / –	0.42
Cu-TCNPP		+0.40	+0.10 [b] / –	–
Cu-*cis*DCNPP + 2 $\mathrm{Cu_{ad}}$		+0.05	– / +0.02	–
Cu-TCNPP + 2 $\mathrm{Cu_{ad}}$		+0.30	+0.12 [c] / +0.03	0.27
Cu-TCNPP + 4 $\mathrm{Cu_{ad}}$		+0.13	– / +0.03	–

[a] An energy cost of 0.03 eV for the porphyrin displacement from the bridge site is included
[b] The strained state of the molecule is not taken into account
[c] The same value as for Cu-*cis*DCNPP is assumed; the remaining part is divided by 2

2) Details on Molecule–Molecule Interactions on Cu(111)

(a) Overview of Cu-TPP network

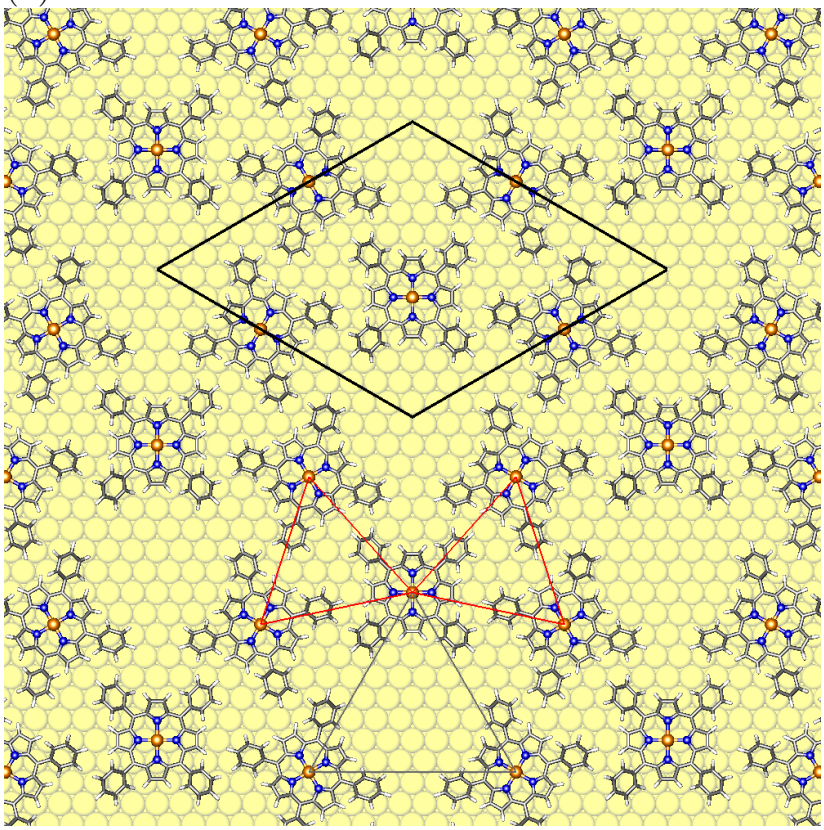

(b) Triangular contact at rim

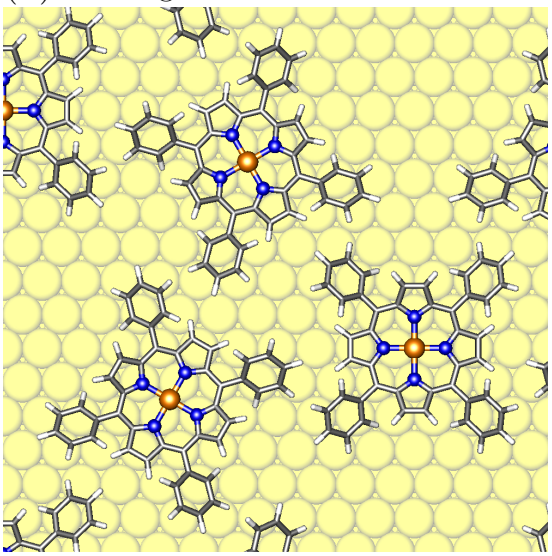

(c) Central pore

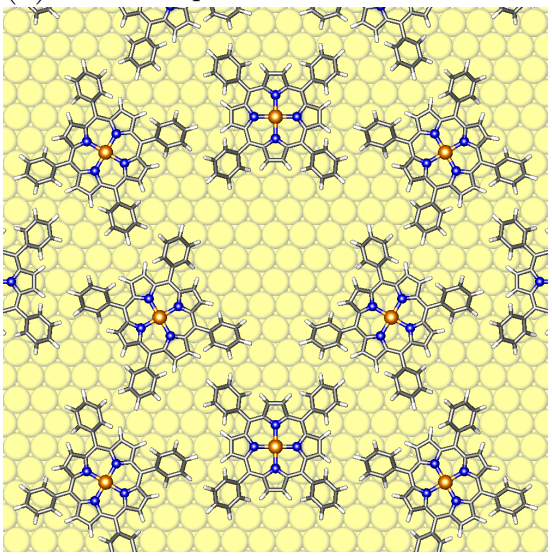

Figure S8: Relaxed structure of three Cu-TPPs in a $(7\sqrt{3}\times7\sqrt{3})$R30° unit cell of the Cu(111) surface (structure **1**). (a) shows an overview of the porous honeycomb-type pattern. The unit cell is indicated by black solid lines. (b) and (c) are enlarged cutouts focusing on the triangular contact at the rim (thin red lines) and the pore structure (thin gray lines), respectively. Both have a 3-fold symmetry axis in their center.

(a) Cu-TPP with no CN groups

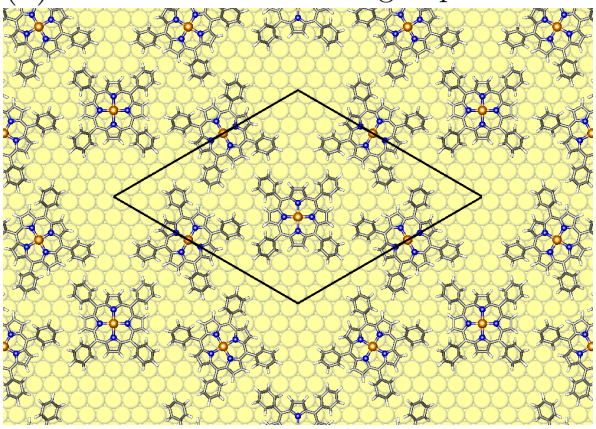

(b) Cu-*cis*DCNPP with CN at rim

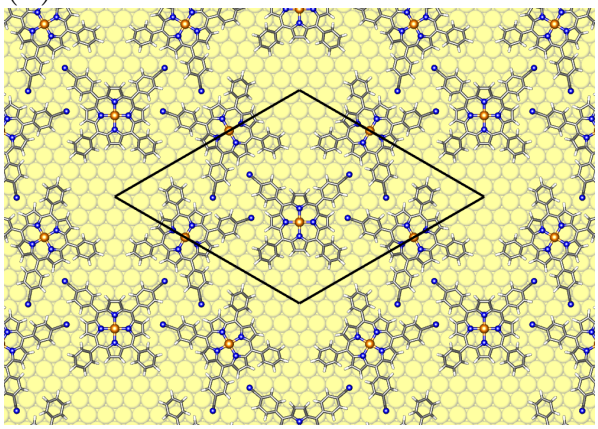

(c) Cu-*cis*DCNPP with CN at pore

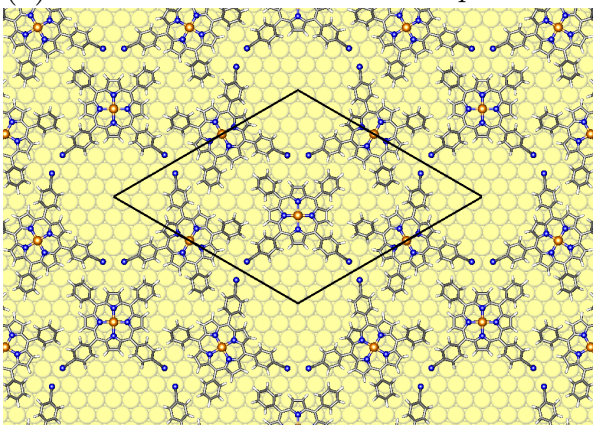

(d) Cu-TCNPP with 4 CN groups

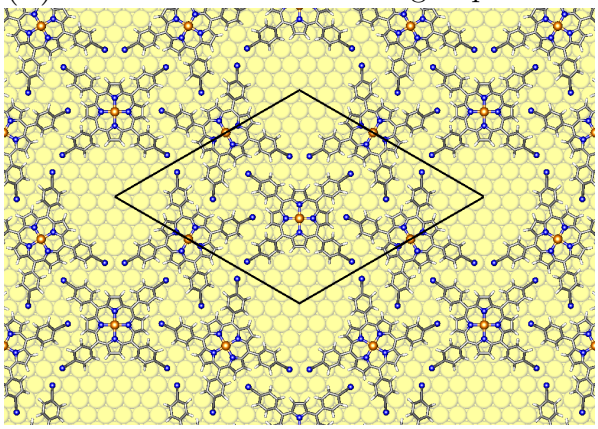

Figure S9: Stepwise addition of CN groups to the ficticious porous honeycomb-type structure of three Cu-TPP molecules in a $(7\sqrt{3}\times7\sqrt{3})$R30° unit cell of the Cu(111) surface. (a) without CN groups (structure **1**), (b) with CN groups at the rim (structure **2**), (c) with CN groups at the pore (structure **3**), and (d) with four CN groups (structure **4**). The unit cell is indicated by black solid lines.

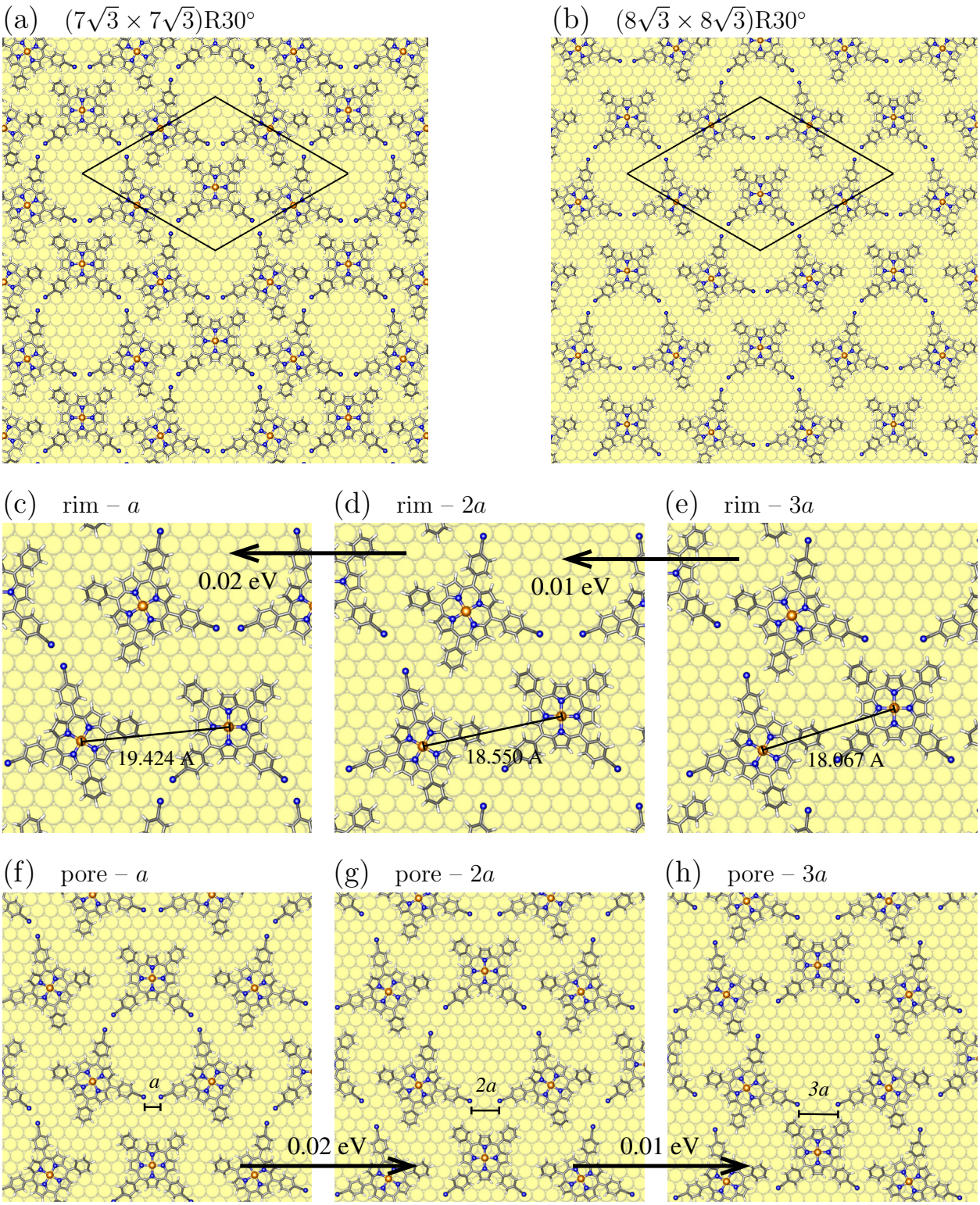

Figure S10: Pore structure motif with Cu-*cis*DCNPP molecules in (a) a $(7\sqrt{3} \times 7\sqrt{3})$R30° (structure **3**) and (b) a $(8\sqrt{3} \times 8\sqrt{3})$R30° unit cell. In the smaller cell, both pore and rim contact are fully established. In the larger cell, the pore can be opened by shifting the porphyrin molecules gradually outwards, thereby closing simultaneously the rim contact. A sequence of the shift, together with the change in the binding energy per molecule, is shown for an enlarged cutout (c-e) of the triangular rim contact and (f-h) of the pore structure. No significant molecule–molecule interactions are present.

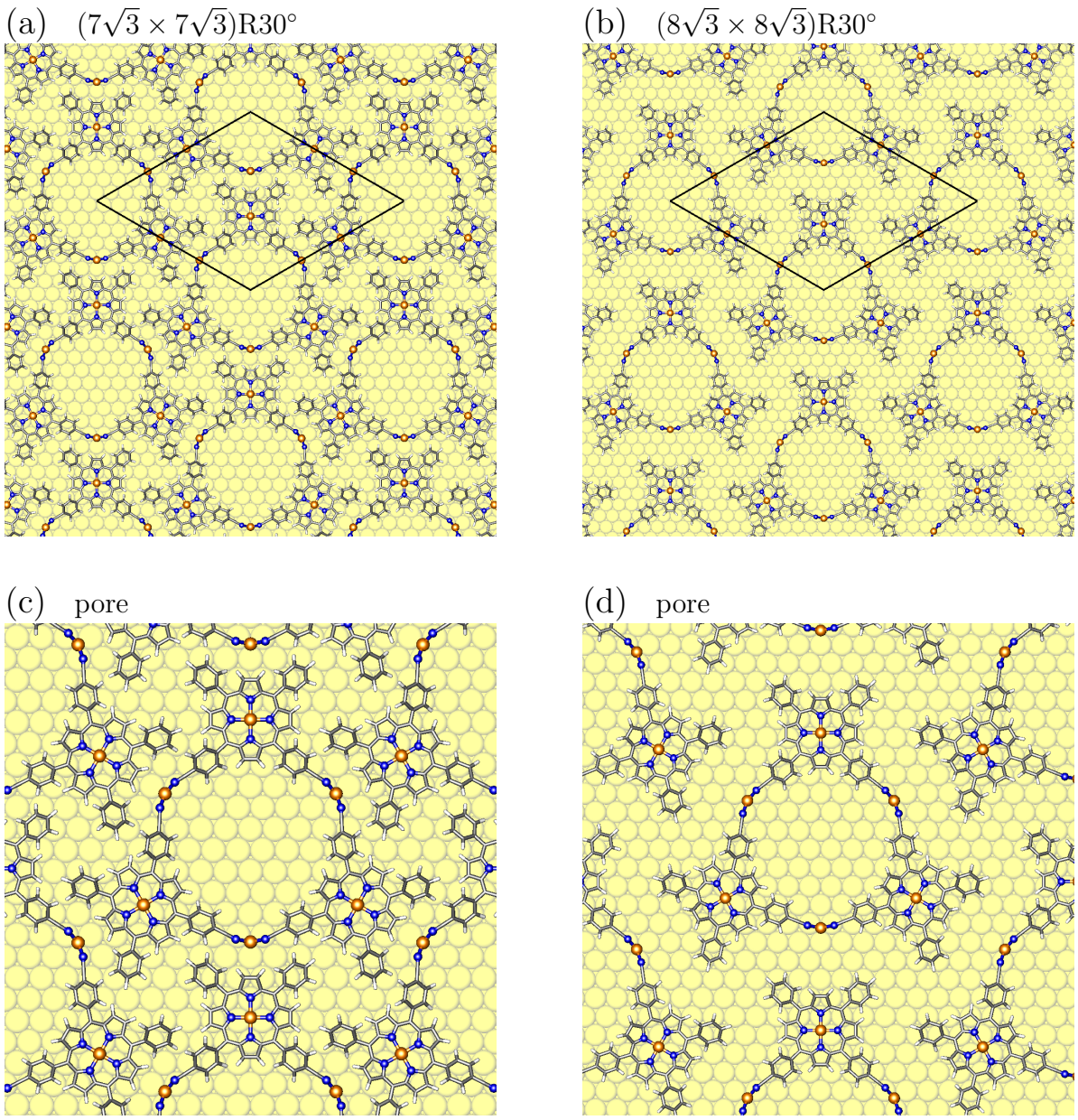

Figure S11: Pore structure motif with Cu-*cis*DCNPP molecules and Cu adatoms in (a) a $(7\sqrt{3} \times 7\sqrt{3})$R30° (structure **5**) and (b) a $(8\sqrt{3} \times 8\sqrt{3})$R30° unit cell with closed and open rim contact, respectively. (c,d) are enlarged cutouts of the pore region. In the smaller unit cell with closed rim contact, the binding energy per molecule is larger by 0.14 eV than for the larger cell with open rim. This is an independent, second estimate for the strength of the molecule–molecule interaction across the rim in the densely-packed configuration (see Table 1 in the manuscript).

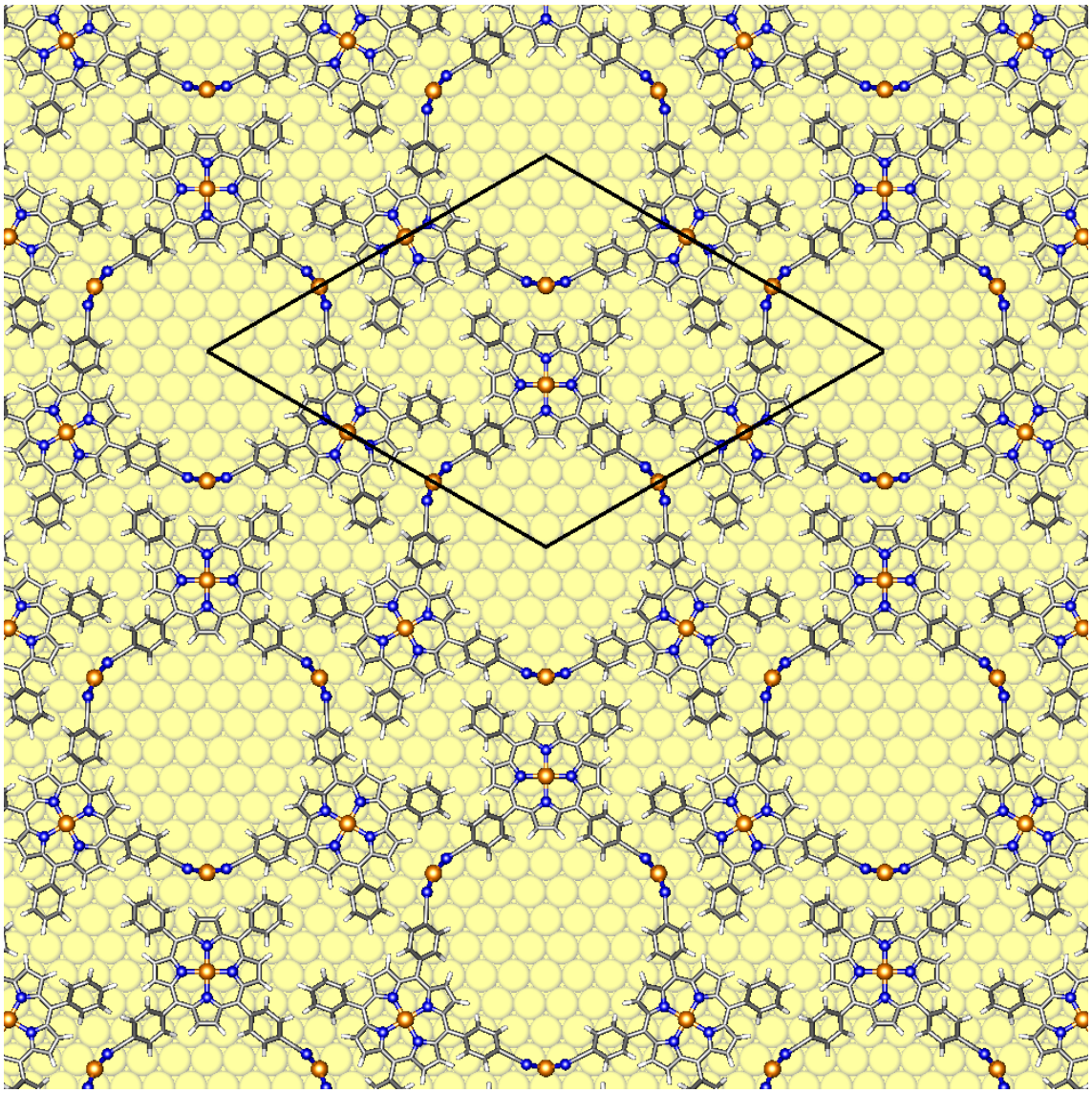

Figure S12: DFT-optimized structure of the porous honeycomb-type network of Cu-*cis*DCNPP porphyrins on Cu(111) (structure **5**). The $(7\sqrt{3} \times 7\sqrt{3})$R30° unit cell with three porphyrin molecules is shown by black solid lines.

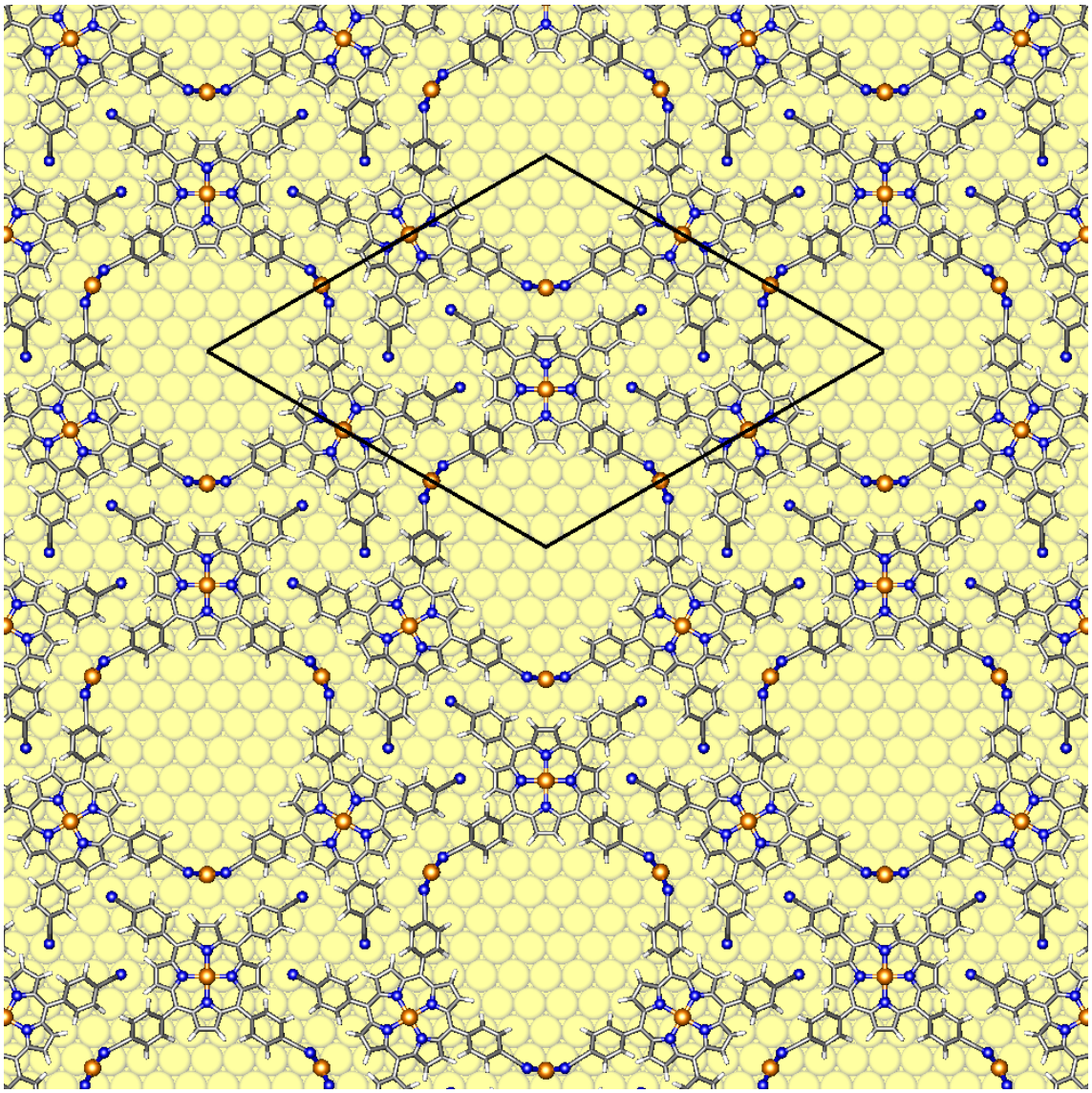

Figure S13: DFT-optimized structure of the porous honeycomb-type network of Cu-TCNPP porphyrins on Cu(111) (structure **6**). The $(7\sqrt{3} \times 7\sqrt{3})$R30° unit cell with three porphyrin molecules is shown by black solid lines.

References

[1] I. Horcas, R. Fernández, J.M. Gómez-Rodríguez, J. Colchero, J. Gómez-Herrero, A.M. Baro, WSXM: A software for scanning probe microscopy and a tool for nanotechnology, *Rev. Sci. Instrum.* **2007**, *78*, 013705.

[2] F. Buchner, E. Zillner, M. Röckert, S. Gläßel, H.-P. Steinrück, H. Marbach, Substrate-Mediated Phase Separation of Two Porphyrin Derivatives on Cu (111), *Chem. Eur. J.* **2011**, *17*, 10226–10229.

[3] M. Lepper, T. Schmitt, M. Gurrath, M. Raschmann, L. Zhang, M. Stark, H. Hölzel, N. Jux, B. Meyer, M.A. Schneider, H.-P. Steinrück, H. Marbach, Adsorption Behavior of a Cyano-Functionalized Porphyrin on Cu(111) and Ag(111): From Molecular Wires to Ordered Supramolecular Two-Dimensional Aggregates, *J. Phys. Chem. C* **2017**, *121*, 26361–26371.

[4] M. Lepper, J. Köbl, L. Zhang, M. Meusel, H. Hölzel, D. Lungerich, N. Jux, A. de Siervo, B. Meyer, H.-P. Steinrück, H. Marbach, Controlling the Self-Metalation Rate of Tetraphenylporphyrins on Cu(111) via Cyano Functionalization, *Angew. Chem.* **2018**, *130*, 10230–10236; *Angew. Chem. Int. Ed.* **2018**, *57*, 10074–10079.

[5] P. Giannozzi, S. Baroni, N. Bonini, M. Calandra, R. Car, C. Cavazzoni, D. Ceresoli, G.L. Chiarotti, M. Cococcioni, I. Dabo, A. Dal Corso, S. de Gironcoli, S. Fabris, G. Fratesi, R. Gebauer, U. Gerstmann, C. Gougoussis, A. Kokalj, M. Lazzeri, L. Martin-Samos, N. Marzari, F. Mauri, R. Mazzarello, S. Paolini, A. Pasquarello, L. Paulatto, C. Sbraccia, S. Scandolo, G. Sclauzero, A.P. Seitsonen, A. Smogunov, P. Umari, R.M. Wentzcovitch, QUANTUM ESPRESSO: A modular and open-source software project for quantum simulations of materials, *J. Phys.: Condens. Matter* **2009**, *21*, 395502.

[6] J.P. Perdew, K. Burke, M. Ernzerhof, Generalized Gradient Approximation Made Simple, *Phys. Rev. Lett.* **1996**, *77*, 3865–3868; Erratum: *Phys. Rev. Lett.* **1997**, *78*, 1396.

[7] D. Vanderbilt, Soft self–consistent pseudopotentials in a generalized eigenvalue formalism, *Phys. Rev. B* **1990**, *41*, 7892–7895.

[8] B.P. Klein, J.M. Morbec, M. Franke, K.K. Greulich, M. Sachs, S. Parhizkar, F.C. Bocquet, M. Schmid, S.J. Hall, R.J. Maurer, B. Meyer, R. Tonner, Ch. Kumpf, P. Kratzer, J.M. Gottfried, The Molecule-Metal Bond of Alternant versus Nonalternant Aromatic Systems on Coinage Metal Surfaces: Naphthalene versus Azulene on Ag(111) and Cu(111), *J. Phys. Chem. C* **2019**, *123*, 29219–29230.

[9] S.R. Kachel, B.P. Klein, J.M. Morbec, M. Schöniger, M. Hutter, M. Schmid, P. Kratzer, B. Meyer, R. Tonner, J.M. Gottfried, Chemisorption and Physisorption at the Metal/Organic Interface: Bond Energies of Naphthalene and Azulene on Coinage Metal Surfaces, *J. Phys. Chem. C*, **2020**, *124*, 8257–8268.

[10] S. Grimme, J. Antony, S. Ehrlich, H. Krieg, A consistent and accurate ab initio parametrization of density functional dispersion correction (DFT-D) for the 94 elements H–Pu, *J. Chem. Phys.* **2010**, *132*, 154104.

[11] S. Grimme, S. Ehrlich, L. Goerigk, Effect of the damping function in dispersion corrected density functional theory, *J. Comput. Chem.* **2011**, *32*, 1456–1465.

[12] M. Lepper, J. Köbl, T. Schmitt, M. Gurrath, A. de Siervo, M.A. Schneider, H.-P. Steinrück, B. Meyer, H. Marbach, W. Hieringer, "Inverted" porphyrins: a distorted adsorption geometry of free-base porphyrins on Cu(111), *Chem. Commun.* **2017**, *53*, 8207–8210.

[13] It is usually assumed that adatoms form by detachment from step edges. However, the energy required for removing a full row of atoms from a step edge (or a full layer of atoms from a surface) is exactly the bulk energy $E_{\mathrm{bulk}}^{\mathrm{Cu}}$.